Available online at www.sciencedirect.com
ScienceDirect
Journal of Hazardous Materials 152 (2008) 994–1001
Journal of Hazardous Materials
www.elsevier.com/locate/jhazmat

Effect of water quenching and SiO_2 addition during vitrification of fly ash Part 1: On the crystalline characteristics of slags

Yi-Ming Kuo [a,*], Jian-Wen Wang [a], Chih-Ta Wang [a], Cheng-Hsien Tsai [b]

[a] *Department of Safety Health and Environmental Engineering, Chung Hwa University of Medical Technology, Tainan County 71703, Taiwan*
[b] *Department of Chemical and Material Engineering, National Kaohsiung University of Applied Sciences, Kaohsiung 80778, Taiwan*

Received 7 March 2007; received in revised form 24 July 2007; accepted 24 July 2007
Available online 28 July 2007

Abstract

The objective of this study is to investigate how cooling rate and basicity in a vitrification process govern the crystalline characteristics of slags. In this experiment, the incineration fly ash mixtures with various SiO_2 addition ratios were vitrified at 1450 °C and cooled down separately by air or water. Different thermal analysis, scanning electron microscopy and X-ray diffraction analysis with an internal standard addition were applied to investigate the crystalline characteristics of slags. The microanalytical mapping images showed that water quenching and the addition of SiO_2, both enhanced the glassy amorphous phase to distribute more uniformly in slags. Addition of SiO_2 would lower the melting temperature of fly ash mixtures and retard the formation of crystalline phases in slags. When the basicity (mass ratio of CaO to SiO_2 before vitrification) was >0.990, the profiles of crystalline phases in slags with equal basicity were similar no matter how they were cooled. However, when the basicity <0.674, water quenching greatly enhanced the formation of the glassy amorphous phase in slags. For air cooled slags, an even lower basicity (<0.511) is required to vitrify fly ash well.

Keywords: Basicity; Crystalline characteristics; Fly ash; Slag; Vitrification

1. Introduction

Waste treatment is an important issue from the environmental protection perspective due to an ever increasing amount of hazardous material which poses a serious threat to public health [1]. Vitrification is regarded as a promising technology to solve these problems and has been successfully applied to treat hazardous materials such as fly ash, sludge or radioactive waste [2–4]. Its major advantage is that the glassy matrix possesses a good chemical stability and can incorporate waste with a complex chemical composition into its vitreous structure [5]. Furthermore, vitrification can afford a significant volume reduction of waste, with evident benefit in terms of storage due to diminishing availability of landfilling sites [6]. It has also been verified that vitrification can homogeneously encapsulate heavy metals into the glassy amorphous matrix and immobilize them [7].

The products of vitrification, including secondary fly ash (removed from the flue gas), slags and ingots, can be separated during the melting process and have a high potential to be utilized as resources [8]. Evaporation orientation metals contained in the secondary fly ash, such as Pb and Zn, can be recovered following a procedure, including extraction by acid, concentration sedimentation and refinement [9]. The ingot can be sent to a smelter to recover Fe or other metals with a large specific weight. The slags are often directly used as building materials such as cement admixture [10] or aggregates for paving, and consequently the long-term stability and chemical durability of slags are extraordinarily important.

Leaching of hazardous metals is highly related to the structure of slags and is shown to be more encouraging in a crystalline structure [11]. This is probably due to the grain boundary precipitation of agglomerates, but no significant evidence supports this assumption. A previous study reported that slow cooling would contribute to the crystallization of slags, whereas rapid cooling would enhance the formation of a glassy amorphous structure [12]. In addition, the basicity (defined as the mass ratio of CaO/SiO_2 before vitrification) has also been found to govern

* Corresponding author. Tel.: +886 6 2674567x854; fax: +886 6 2675049.
E-mail address: yiming@mail.hwai.edu.tw (Y.-M. Kuo).

0304-3894/$ – see front matter © 2007 Elsevier B.V. All rights reserved.
doi:10.1016/j.jhazmat.2007.07.081

the crystalline characteristics of slag structures [13]. It stands to reason that the cooling rate and basicity considerably affect the leaching behavior of metal species. Nevertheless, how these two factors govern the process of vitrification has not been further investigated.

The object of this study is to evaluate the influence of cooling rate and basicity on the characteristics of slags. Two sections were conducted in this investigation—part 1: crystalline characteristics and part 2: chemical stability/acid resistance. Part 1 attempted to determine the amount of crystalline phases of slags with various basicities and cooling rates. The influence of these two factors on the distribution of elements and the formation of slag structures were also investigated together.

2. Experimental Section

2.1. Sampling and preparation

The fly ash used in this experiment was sampled from fabric filters in air pollution control devices at a municipal solid waste incinerator located in southern Taiwan. Crystallized SiO_2 (quartz) served as an additive to adjust the basicity of fly ash with SiO_2/fly ash (S/A) mass mixing ratios of 0, 0.1, 0.2, 0.3 and 0.4, denoted as Ash-0, Ash-1, Ash-2, Ash-3 and Ash-4, respectively. Ash mixtures were heated to 1450 °C with a heating rate of 6 °C/min. Specimens were then cooled by air cooling or water quenching. The air-cooled or water-quenched slags were labeled with such as A0–A4 and W0–W4, respectively.

2.2. Estimation of metal content in specimens

The slags and fly ash were pulverized to the size that passed through a mesh 100 sieve to ensure uniform digestion efficiency. All samples with a 0.5 g weight were digested with an acid mixture (1 mL HBF_4 + 5 mL HNO_3 + 10 mL HCl) in a hermetically sealed Teflon tube at 180 °C for 1 h. The digestion solution was diluted to exactly 25 mL, filtrated by a 0.8 cellulose ester filter, and then analyzed. An inductively coupled plasma atomic emission spectrometry (Jobin Yvon JY-38 Plus ICP-AES) was applied to analyze the metal species, including Al, Ca, Cd, Cu, Cr, Fe, Mg, Mn, Ni, Pb, Si, and Zn, in sample digests to estimate the metal composition of the slags and the fly ash. The basicity of specimens can be calculated by the following equation:

$$\text{basicity} = \frac{\text{CaO}}{\text{SiO}_2} = \frac{[\text{Ca}] \times 56/40}{[\text{Si}] \times 60/28}$$

[Ca]: content of Ca (%) in the ash mixture before vitrification; [Si]: content of Si (%) in the ash mixture before vitrification.

2.3. Evaluation of crystalline and surface characteristics of slags

Different thermal analysis (DTA) and thermogravimetric analysis (TGA) were utilized to measure the glass thermal property and mass loss of the specimens, respectively. The analysis was performed by a differential thermal analyzer (Setaram Setsys-Evolution-1600, France) with ash mixtures in platinum

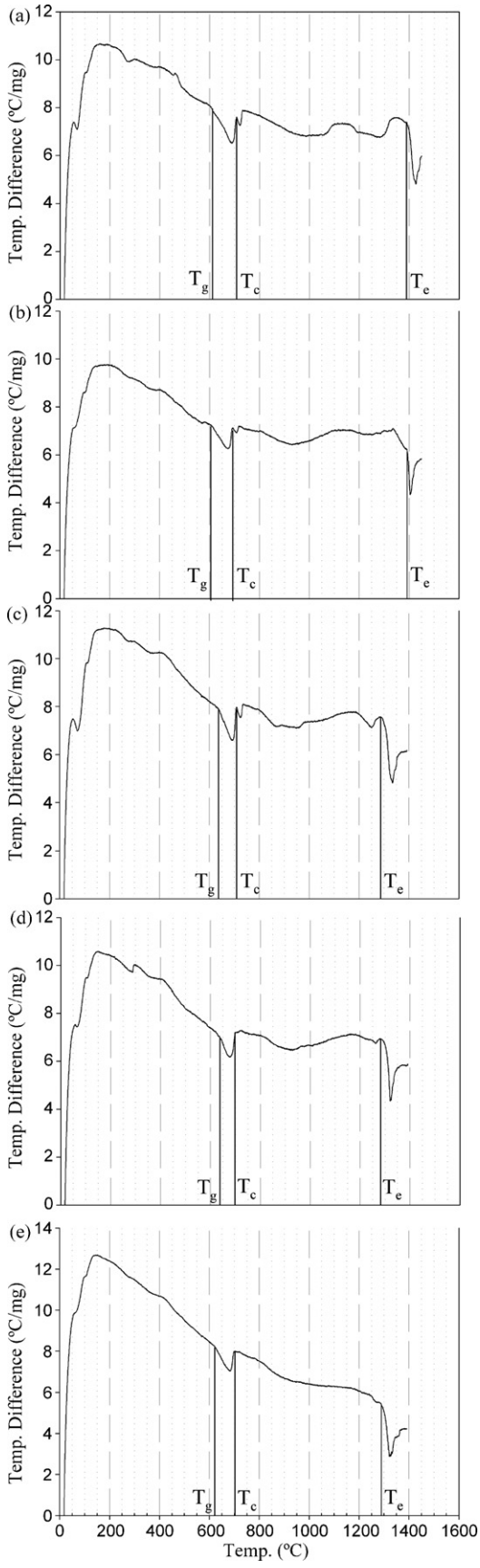

Fig. 1. DTA curves of ash mixtures (a) Ash-0, (b) Ash-1, (c) Ash-2, (d) Ash-3 and (e) Ash-4.

Table 1
Composition of fly ash and slags ($n = 3$)

Crust elements	Ash-0			A-0				W-0			
	Range (%)	Average (%)	R.S.D. (%)	Range (%)	Average (%)	R.S.D. (%)	PMR	Range (%)	Average (%)	R.S.D. (%)	PMR
Al_2O_3	0.604–0.711	0.671	8.62	1.16–1.40	1.31	10.4	1.11	1.12–1.29	1.22	6.87	1.03
CaO	19.4–23.0	21.1	8.44	39.4–43.2	40.7	5.30	1.09	34.3–38.0	35.9	5.32	0.967
Fe_2O_3	1.63–2.05	1.82	11.6	2.99–3.16	3.07	2.80	0.955	2.61–2.71	2.65	1.86	0.826
MgO	0.918–1.03	0.972	6.01	1.63–1.72	1.66	2.86	0.969	1.63–1.67	1.65	1.34	0.961
SiO_2	0.757–1.60	1.31	36.6	2.05–2.25	2.15	4.65	0.929	1.81–2.27	2.10	11.9	0.909
Anthropogenic metals	Ash-0			A-0				W-0			
	Range (mg/kg)	Average (mg/kg)	R.S.D. (%)	Range (mg/kg)	Average (g/kg)	R.S.D. (%)	PMR	Range (mg/kg)	Average (g/kg)	R.S.D. (%)	PMR
Cd	35.2–38.7	36.8	4.80	3.52–4.32	3.80	11.8	0.059	6.62–6.67	6.64	0.38	0.102
Cr	470–573	508	11.1	332–360	348	4.19	0.388	353–370	364	2.64	0.406
Cu	253–300	276	8.46	607–645	626	3.06	1.28	403–422	412	2.23	0.846
Mn	283–352	311	11.7	458–478	471	2.36	0.860	455–468	461	1.46	0.841
Ni	14.4–28.7	21.2	33.9	123–132	127	3.53	3.39	42.7–54.0	48.0	11.9	1.28
Pb	2400–2520	2470	2.55	1250–1360	1300	4.56	0.298	1170–1310	1230	5.99	0.281
Zn	5150–7320	6110	18.1	48.7–60.3	53.3	11.6	0.005	54.2–73.3	65.1	15.2	0.006

R.S.D.: relative standard deviation.

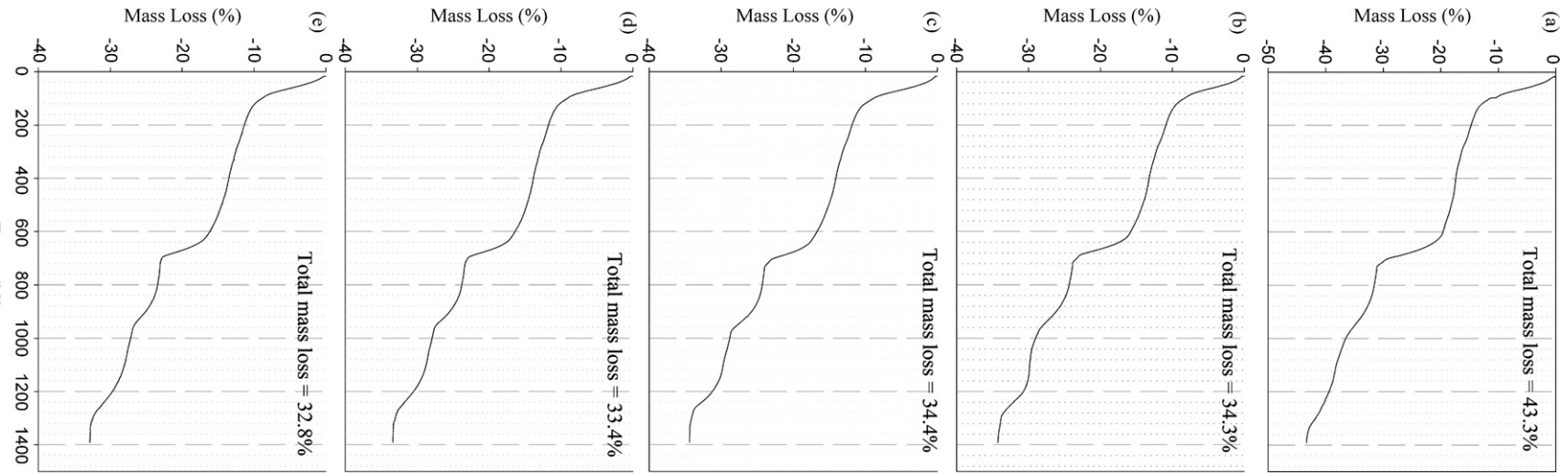

Fig. 2. TGA curves of ash mixtures (a) Ash-0, (b) Ash-1, (c) Ash-2, (d) Ash-3 and (e) Ash-4.

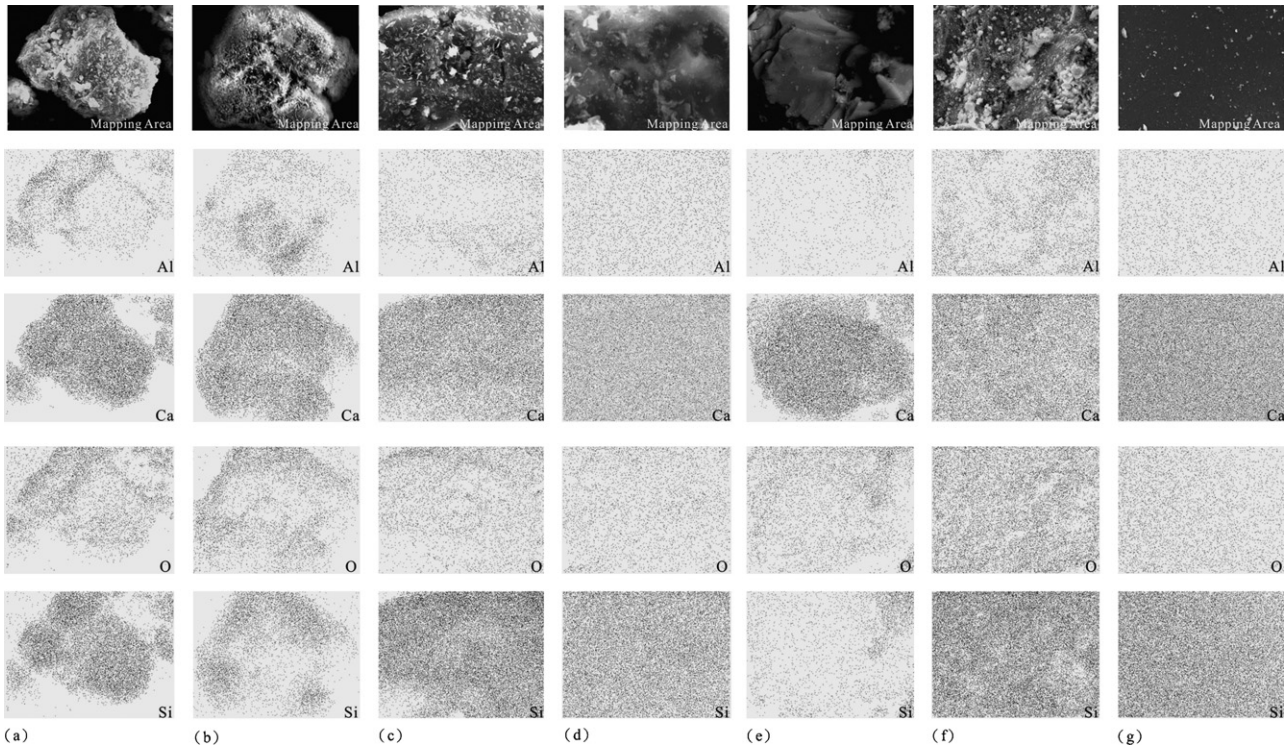

Fig. 3. Microanalytical mapping images of Al, Ca, O and Si in specimens (a) Ash-0, (b) A-0, (c) A-2, (d) A-4, (e) W-0, (f) W-2 and (g) W-4.

crucibles using a heating rate of 10 °C/min. The composition of metal and the mass loss of specimens were used to evaluate percent mass retained (mass retained in the slag/mass in the ash mixture, PMR) of the metal species during vitrification. In addition, three notable temperatures, including T_g, T_c, and T_e, were marked on the DTA curves. The definitions and characteristics of these temperatures are described in the next paragraph.

I. T_g (glass transition temperature): It is a temperature below which the physical properties of amorphous materials vary in a manner similar to those of a crystalline phase (glassy state), and above which amorphous materials behave like liquids (rubbery state). It is also the mid-point of a temperature range (usually at 600–700 °C) in which the materials gradually become more viscous and change from being liquid to solid.
II. T_c (crystallization temperature): Above this temperature, a crystallization process which consists of nucleation and crystal growth will occur in the specimen. During this process, a sharp exothermic peak (usually between 700 and 800 °C) on the DTA figure could be clearly observed.
III. T_e (liquid temperature): Liquid temperature is the temperature at which the specimen changes from solid to liquid state. It represents the temperature for the dissolution or melting of crystals, and is usually above 1200 °C.

Scanning electron microscopy—energy dispersive spectroscopy (Jeol JXA-840 SEM-EDS) was applied to examine the distribution of the elements on the surface by a mapping microanalysis. Pulverized specimens (<74 μm) were adhered on a metallic plate, coated with Au using an ion sputter coater, and then scanned by microscopy.

The crystalline phases in slags were determined by X-ray diffraction (XRD) analysis. It was carried out by a powder diffractometer (Geigerflex 3063) with Ni-filtered Cu Kα radiation on powders, at particle size <20 μm, at 4°/min^{-1}, in the $2\theta = 10$–60° range. Crystalline phases were identified by comparing intensities and positions of Bragg peaks with those listed in the Joint Committee on Powder Diffraction Standards (JCPDS) data files.

In this work, the volume fraction of the crystalline phase in slags was measured by an XRD analysis with an internal standard addition [14]. High-purity silica was used to mix with specimens as an internal standard with a Si/sample mass ratio of 0.1. It served as a reference material in the crystalline quantitative analysis. The approximate fraction of the crystalline phase was then determined according to the area of their specific peaks in comparison with the internal standard and the details of the procedure given in a previous report [15].

3. Result and discussion

3.1. Characteristics of fly ash and slags

Fig. 1 shows the DTA curves, on which T_g, T_c, T_e, and the mass losses of specimens are marked. Addition of SiO_2 enhanced T_g and T_e to shift to a lower temperature, but had no significant effect on the shift of T_c. However, as the S/A increased to 0.3, the exothermic peak of T_c almost disappeared. Obviously, the addition of SiO_2 increased the amount of glassy amorphous phase in slags. The glass transition during vitrifica-

tion was consequently promoted, causing the lowering of T_g. According to the Al_2O_3–CaO–SiO_2 ternary phase diagram, the addition of SiO_2 in a silica-deficient condition for vitrification would also lower its melting temperature, supporting the drop of T_e in the DTA figures.

Our previous study has shown that SiO_2 addition during vitrification will promote the formation of an amorphous phase, in other words, retard the crystallization. Therefore, the peak of crystallization temperature would gradually diminish as more SiO_2 is added. The shift and diminishing behavior of temperature peaks in DTA curves offer preliminary verification that the SiO_2 addition enhances the formation of a glassy amorphous phase and promotes the vitrification process.

3.2. Metal content in fly ash and slags

The metal components of fly ash and slags (A-0 and W-0 as representative of air cooled and water quenching slags) are shown in Table 1. The metal content (except for Si) in A-1 to A-4 and W-1 to W-4 decrease proportionally due to the addition of SiO_2. The ternary major glassy matrix elements in fly ash, Al_2O_3, CaO and SiO_2, were 0.671, 21.1 and 1.31%, respectively. The reason for the extremely high CaO content in the fly ash was that the air pollution control device involved used $Ca(OH)_2$ as an additive to remove acidic pollutants in the flue gas. This also caused the high basicity (basicity = 16.1) of the pure fly ash, which was thus not favorable for vitrification. The major anthropogenic metals were Pb (2470 mg/kg), Zn (6110 mg/kg), Cr (508 mg/kg) and Cu (276 mg/kg), commonly seen in fly ash from other sources [16]. After vitrification, the contents of Al_2O_3, CaO, Cr, Cu Fe_2O_3, MgO, Mn, Ni, and SiO_2 in A-0 and W-0 were all elevated to roughly two times of those in Ash-0. The results of TGA are illustrated in Fig. 2 on which the total mass losses of specimens are marked. The PMRs (all were ~1) which were calculated according to the total mass loss and metal content of specimens indicated that these metal species were mostly retained in the slags and this could also explain why the content was elevated after vitrification. In contrast, the composition of Cd, Pb and Zn was drastically reduced due to the vaporization of metals during vitrification. The residual fractions of these metals were trapped in the secondary fly ash or exhausted into the flue gas, findings which were verified in our previous study [17]. The metal behaviors of both retained and vaporized species during vitrification were all similar to the result of a previous study [7]. In addition, the similarity of composition of A-0 and W-0 also revealed that the cooling rate would not noticeably affect the composition of slags.

3.3. Distributions of elements on the surface of specimens

Fig. 3(a–g) displayed the microanalytical mapping images of the fly ash, air cooled slags and water quenched slags. Obviously, Ca distributed very uniformly and densely on the surface of all specimens. In Fig. 3(b), Al and O gathered more densely in some regions of A-0 which were complementary to Si. In comparison to its mapping image, this indicated that the composition of the crystalline phase on the surface of slags was predominately Ca, Al and O, instead of Si. For A-2, Si and O presented a more uniform distribution, whereas Al was still distributed more densely in some regions. For A-4, all elements dispersed more uniformly and no obvious aggregations were found in the mapping area. In Fig. 3(e and f), no noticeable aggregations of elements were found, but only some defects were observed in the distribution of Al, O and Si, which matched the aggregates on the surface of slags (on the image of mapping area). This indicated that the aggregates were composed of Ca and other trace elements, instead of the glassy matrix elements of slag. As for W-4, all elements showed a dense and uniform distribution, which made it clear that water quenching and addition of SiO_2 would both enable Al and O to disperse more uniformly during vitrification. Fig. 4(a and b) illustrates the mapping images of Fe in W-2 and W-3. Some aggregates were observed and this revealed the segregation of Fe caused by the gravity effect during vitrification [17]. With enough amounts of high specific weight metals, they will be separated into the bottom of specimens as ingot.

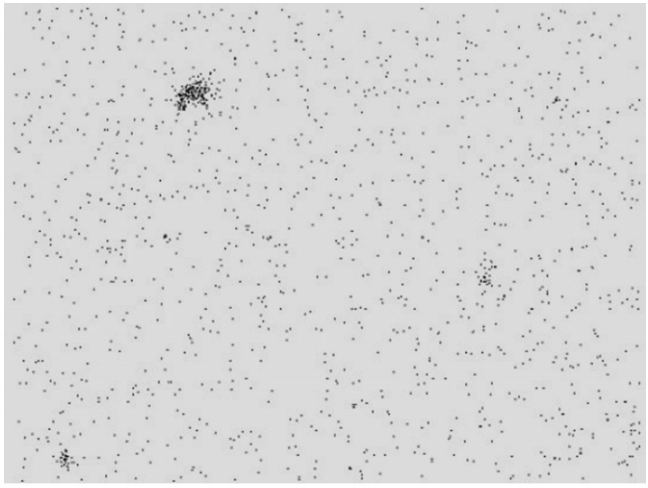
(a)

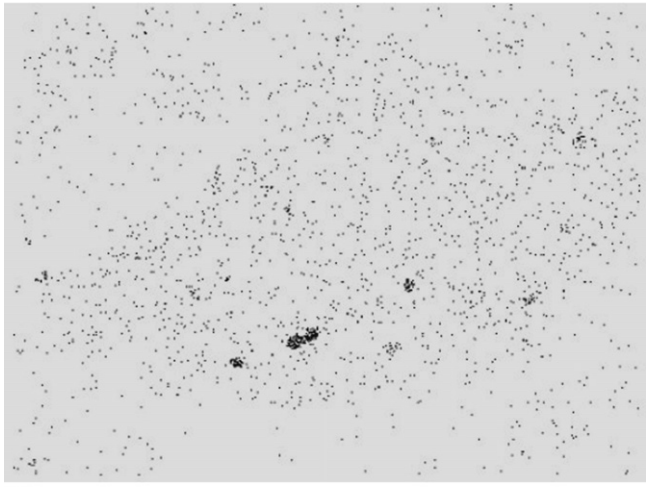
(b)

Fig. 4. Microanalytical mapping images of Fe in slags (a) W-2 and (b) W-3.

According to the mapping microanalysis, the distribution of glass matrix elements, including Al, Ca, O, and Si, can

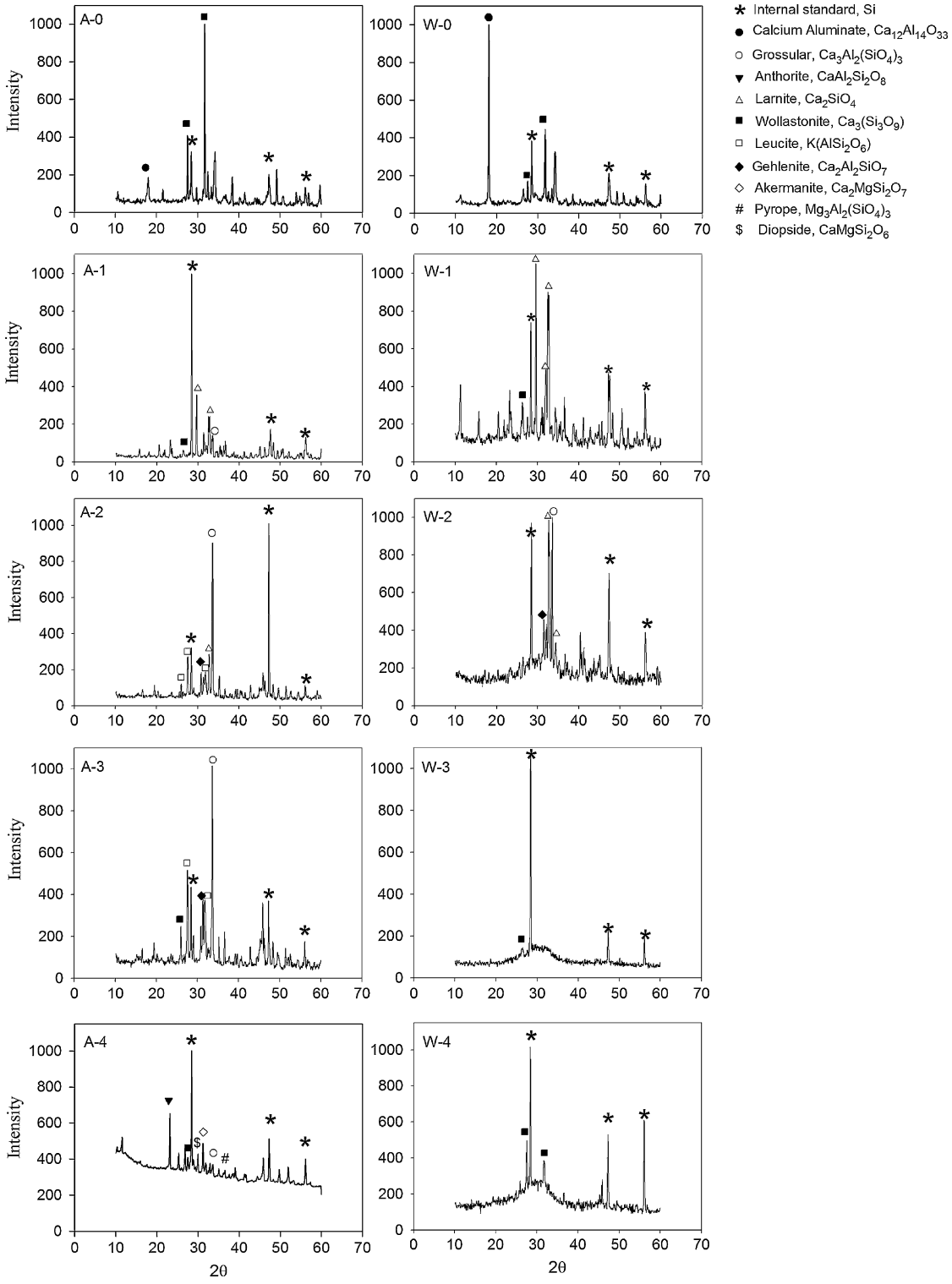

Fig. 5. XRD analysis patterns of slags.

represent the distribution of the glassy phase on the slag surface. Therefore, the defectiveness of these elements on the mapping graph revealed that these areas were not well encapsulated by the glassy amorphous phase. Thus, hazardous metals depositing on these un-encapsulated areas would be easily leached out due to the grain boundary precipitation. The distribution of Al, O, and Si were more uniform in water quenched slags with higher SiO_2 addition ratio. From this viewpoint, the statement could be made with fair certainty that water quenching and SiO_2 addition could enhance a more uniform distribution of the glassy amorphous phase in slags. This can also explain the reason why leaching of hazardous metals is more likely in a crystalline than an amorphous structure.

Table 2
Crystalline characteristics of slags with various basicity and cooling method

Specimen	Basicity	Crystalline phase	Volume fraction (%)	Crystalline phase	Volume fraction (%)
A-0	16.1	Wollastonite, $Ca_3(Si_3O_9)$	12.5	Calcium Aluminate $Ca_{12}Al_{14}O_{33}$	3.06
A-1	1.87	Larnite, Ca_2SiO_4	6.00	Grossular, $Ca_3Al_2(SiO_4)_3$	1.42
A-2	0.990	Grossular, $Ca_3Al_2(SiO_4)_3$	8.17	Leucite, $KAlSi_2O_6$	6.45
A-3	0.674	Grossular, $Ca_3Al_2(SiO_4)_3$	13.7	Leucite, $KAlSi_2O_6$	10.5
A-4	0.511	Anorthite, $CaAl_2Si_2O_8$	3.08	Akermanite, $Ca_2MgSi_2O_7$	1.92
W-0	16.1	Calcium Aluminate, $Ca_{12}Al_{14}O_{33}$	10.4	Wollastonite $Ca_3(Si_3O_9)$	6.69
W-1	1.87	Larnite, Ca_2SiO_4	15.0	Wollastonite $Ca_3(Si_3O_9)$	1.88
W-2	0.990	Larnite, Ca_2SiO_4	7.49	Grossular, $Ca_3Al_2(SiO_4)_3$	3.92
W-3	0.674	Wollastonite, $Ca_3(Si_3O_9)$	0.88	–	–
W-4	0.511	Wollastonite, $Ca_3(Si_3O_9)$	3.89	–	–

3.4. Characteristics of crystalline phases in slags

Fig. 5 illustrates the XRD analysis diagrams and crystalline phases of slags, and the crystalline characteristics of slags are shown in Table 2. The predominant crystalline phases of A-0 and W-0 were both Wollastonite [$Ca_3(Si_3O_9)$] and Calcium Aluminate ($Ca_{12}Al_{14}O_{33}$), but varied in their amounts. For A-1 and W-1, the major crystalline phase of both was Larnite (Ca_2SiO_4). However, the predominant crystalline phase in A-2 and W-2 was not completely the same, although Larnite (Ca_2SiO_4), Grossular [$Ca_3Al_2(SiO_4)_3$] and Gehlenite ($Ca_2Al_2SiO_7$) were found in these two slags from the XRD analysis.

In comparison to the XRD diagrams of A-0/W-0, A-1/W-1 and A-2/W-2, identical but various amounts of crystalline phases were found in these slag pairs. Therefore, it demonstrated that the profiles of crystalline phases in slags with the same basicity were similar at a basicity >0.990, no matter how the slags were cooled.

As for W-3 and W-4, the major crystalline phase was Wollastonite [$Ca_3(Si_3O_9)$] but the amounts were both <5%. In A-3, the amounts of Grossular, [$Ca_3Al_2(SiO_4)_3$] and Leucite, [$KAlSi_2O_6$] were 13.7 and 10.5%. Meanwhile, for A-4, the amounts of Anorthite, [$CaAl_2Si_2O_8$] and Akermanite, [$Ca_2MgSi_2O_7$] were 3.08 and 1.92%, respectively. This clearly indicated that W-3 and W-4 were well vitrified and no significant crystalline phase was detected. In contrast, the growth of crystalline phases was still encouraged in A-3 but was reduced in A-4. This study showed that either lower basicity or water quenching would retard the formation of crystalline phases. Nevertheless, the effect of vitrification could be achieved completely only on the condition that slags were cooled by water quenching with a basicity <0.674. For air cooled slags, an even lower basicity (<0.511) was required to vitrify fly ash well.

4. Conclusion

Addition of SiO_2 would lower the glass transition temperature of fly ash mixture due to the increase in the amount of glassy phase. It also reduced the peak height of crystallization temperature in the DTA curves, revealing a retardation of the crystalline phase formation in slags. In addition, water quenching also improved the effect provided that enough SiO_2 is added during vitrification. When the basicity was >0.990, the profiles of crystalline phases in slags with equal basicity were similar no matter how they were cooled. However, when basicity <0.674, drastically different structure between air cooled and water quenched slags could be clearly observed. This suggests out that water quenching plays as a critical role, at the basicity <0.674, to enhance the formation of glassy amorphous phase in slags. For air cooled slags, a basicity <0.511 is required to vitrify fly ash well. Lower basicity and water quenching would both enhance Al, Si, and O to disperse more uniformly in slags. The addition of SiO_2 can increase the amount of glassy phase and hence make Si distribute more densely in slags. This kind of distribution of these glass matrix elements means a uniform encapsulation of the glassy phase in slag, and also potentially a better immobilization of hazardous metals.

References

[1] L. Reijnders, Disposal, uses and treatments of combustion ashes: a review, Resour. Conserv. Recycl. 43 (2005) 313–336.
[2] Y.M. Kuo, T.C. Lin, P.J. Tsai, W.J. Lee, H.Y. Lin, Fate of polycyclic aromatic hydrocarbons during vitrification of incinerator ash in a coke bed furnace, Chemosphere 51 (2003) 313–319.
[3] P. Kanchanapiyaa, T. Sakanoa, C. Kanaokab, T. Mikunia, Y. Ninomiyac, L. Zhangc, M. Masuid, F. Masamia, Characteristics of slag, fly ash and deposited particles during melting of dewatered sewage sludge in a pilot plant, J. Environ. Manage. 79 (2006) 163–172.
[4] P. Hrma, J.V. Crum, D.J. Bates, P.R. Bredt, L.R. Greenwood, H.D. Smith, Vitrification and testing of a Hanford high-level waste sample. Part 1: glass fabrication, and chemical and radiochemical analysis, J. Nucl. Mater. 345 (2005) 19–30.
[5] Y.M. Kuo, T.C. Lin, P.J. Tsai, Immobilization and encapsulation during vitrification of incineration ashes in a coke bed furnace, J. Hazard. Mater. B133 (2006) 75–78.
[6] H. Ecke, H. Sakanakura, T. Matsuto, N. Tanaka, A. Lagerkvist, Effect of electric arc vitrification of bottom ash on the mobility and fate on metals, Environ. Sci. Technol. 35 (2001) 1531–1536.
[7] Y.M. Kuo, T.C. Lin, P.J. Tsai, Effect of SiO_2 on immobilization of metals and encapsulation of a glass network in slag, J. Air Waste Manage. 53 (2003) 1412–1416.
[8] E. Ecke, H. Sakanakura, T. Matsuto, N. Tanaka, A. Lagerkvist, State of the art treatment processes for municipal solid waste incineration residues in Japan, Waste Manage. Res. 18 (2000) 41–51.
[9] D. Kuchar, T. Fukuta, M.S. Onyango, H. Matsuda, Sulfidation treatment of molten incineration fly ashes with Na_2S for zinc, lead and copper resource recovery, Chemosphere 67 (2007) 1518–1525.
[10] K. Kakimoto, Y. Nakano, T. Yamasaki, K. Shimizu, T. Idemitsu, Use of fine-grained shredder dust as a cement admixture after a melting, rapid-cooling and pulverizing process, Appl. Energy 79 (2004) 425–442.

[11] Y.J. Park, J. Heo, Vitrification of fly ash from municipal solid waste incinerator, J. Hazard. Mater. B91 (2002) 83–93.
[12] K.E. Haugsten, B. Gustavson, Environmental properties of vitrified fly ash from hazardous and municipal waste incineration, Waste Manage. 20 (2000) 167–176.
[13] C.T. Li, Y.J. Huang, K.L. Huang, W.J. Lee, Characterization of slags and ingots from the vitrification of municipal solid waste incineration ashes, Ind. Chem. Eng. Res. 42 (2003) 2306–2313.
[14] B.D. Cullity, S.R. Stock, Elements of X-ray Diffraction, third ed., Prentice Hall, Upper Saddle River, 2001.
[15] C.Y. Chen, G.S. Lan, W.H. Tuan, Preparation of mullite by the reaction sintering of kaolinite and alumina, J. Eur. Ceram. Soc. 20 (2000) 2519–2525.
[16] K.L. Lin, C.T. Chang, Leaching characteristics of slag from the melting treatment of municipal solid waste incinerator ash, J. Hazard. Mater. B135 (2006) 296–302.
[17] Y.M. Kuo, T.C. Lin, P.J. Tsai, Metal behavior during vitrification of incinerator ash in a coke bed furnace, J. Hazard. Mater. B109 (2004) 79–84.